

50

ИНСТИТУТ ЯДЕРНОЙ ФИЗИКИ  
СО АН СССР

A.D.Bukin, I.B.Vasserman, L.M.Kurdadze,  
M.Yu.Lelchuk, V.A.Sidorov, A.N.Skrinsky,  
A.G.Chilingarov, Yu.M.Shatunov, B.A.Shwartz,  
S.I.Eidelman

OBSERVATION OF  $\Phi \rightarrow \pi^+ \pi^-$  DECAY

ПРЕПРИНТ ИЯФ 79-66

Новосибирск

OBSERVATION OF  $\Phi \rightarrow \pi^+\pi^-$  DECAY

A.D.Bukin, I.B.Vasserman, L.M.Kurdadze,  
M.Yu.Lelchuk, V.A.Sidorov, A.N.Skrinsky,  
A.G.Chilingarov, Yu.M.Shatunov, B.A.Shwartz,  
S.I.Eidelman

Institute of Nuclear Physics  
630090, Novosibirsk-90, USSR

A b s t r a c t

The interference connected with the  $\Phi(1020) \rightarrow \pi^+\pi^-$  decay has been observed in the process  $e^+e^- \rightarrow \pi^+\pi^-$ . Optimal values for decay parameters are:

$$B(\Phi \rightarrow \pi\pi) = 1.0_{-.5}^{+.8} \cdot 10^{-4}$$

$$\psi = -13^\circ \pm 20^\circ$$

Submitted to the International Symposium  
on Lepton and Photon Interaction,  
Batavia, USA, 1979

Figure captions

Fig. 1. The detector "OLYA".

Fig. 2. a) - The excitation curve of the  $\Phi$  - meson in reactions  $e^+e^- \rightarrow \Phi \rightarrow K_L K_S \rightarrow \pi^+ \pi^-$

and  $e^+e^- \rightarrow \Phi \rightarrow \pi^+ \pi^- \pi^0$

used for absolute calibration of the energy scale in one scanning cycle.

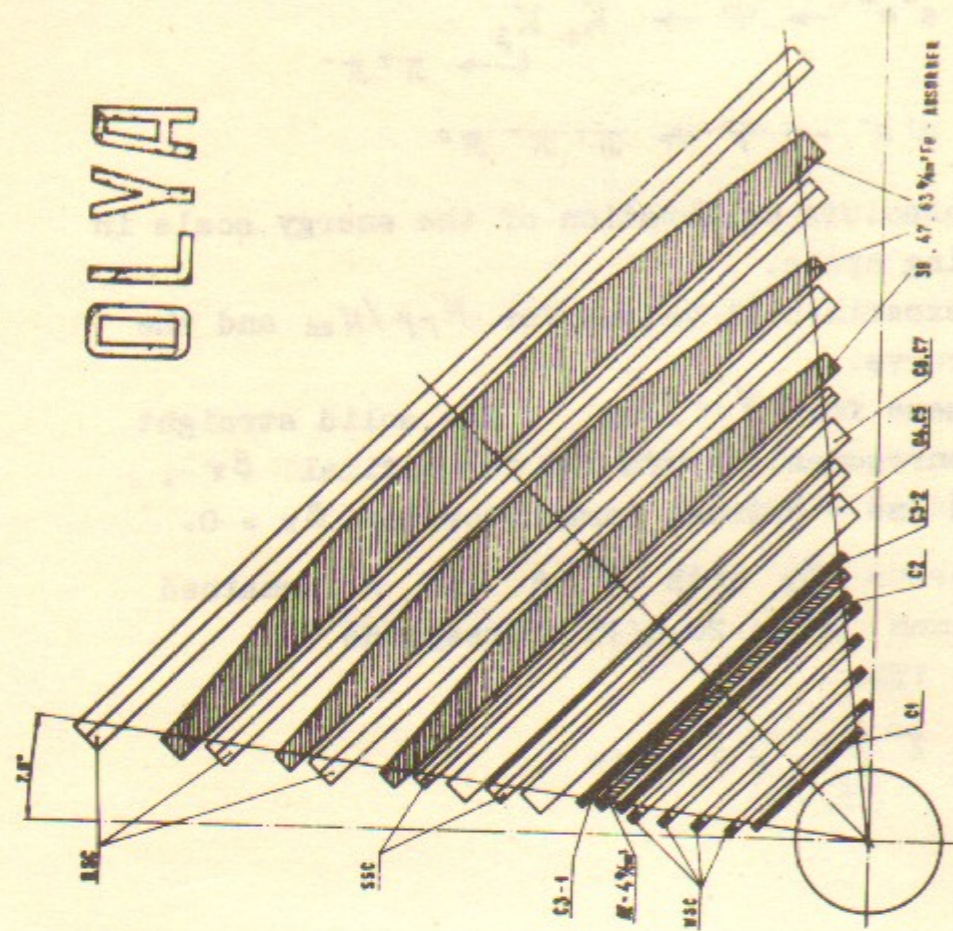
b) - The experimental values for  $N_{\mu\mu}/N_{ee}$  and the best fit curve.

c) - The same for  $N_{\pi\pi}/N_{ee}$ . The solid straight line is nonresonant formfactor for optimal  $B_\pi$ , the dashed one - optimal formfactor for  $B_\pi = 0$ .

Fig. 3. The  $\chi^2$  versus  $B_\pi$  with  $\Psi, A$  and  $K$  remained free. Minimum  $\chi^2 = 20.5/15$  corresponds to  $P(\chi^2) = 15\%$ .

$$\Delta \chi^2 \Big|_{B_\pi=0} = 9 \text{ units}$$

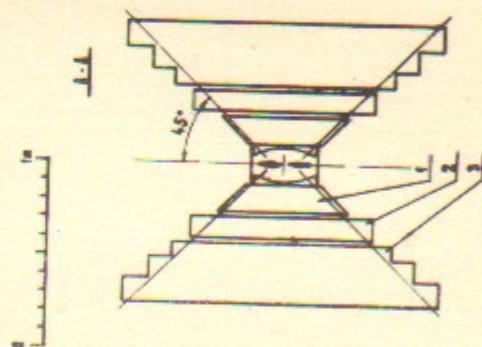
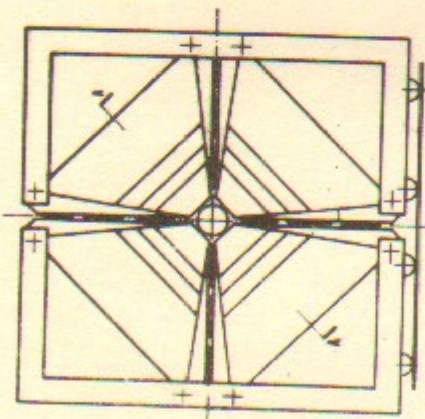
OLYA



MSC - WIRE SPARK CHAMBERS  
SSC - SHOWER SPARK CHAMBERS  
RSC - RANGE SPARK CHAMBERS

C1, C2 - TRIGGER COUNTERS  
C1, C2 - T. O. F.  
C3, C4, C5, C6, C7 - SHOWER COUNTERS

Fig 1.



1 - COORDINATE CHAMBERS  
2 - SHOWER DETECTOR  
3 - RANGE SYSTEM

ground was that provided two pions from  $K_S$  decay were collinear one of them had the energy close to the lowest possible  $E_{\min} = 210$  MeV. Such a pion stopped in the first sandwich and with almost 100% probability gave no signal in the shower-range spark chambers. Therefore, in the present analysis we demanded that both detected particles fired at least one of shower-range chambers along their track directions. This cut eliminated about 25% of the main  $\pi^+ \pi^-$  effect but the  $K_S \rightarrow \pi^+ \pi^-$  contamination went down to  $\sim .1\%$  of  $\pi^+ \pi^-$ . The process  $e^+ e^- \rightarrow \varphi \rightarrow \pi^+ \pi^- \pi^0$  added less than .2% to collinear  $\pi^+ \pi^-$ . The  $e^+ e^-$  electroproduction at large angles could imitate  $\pi^+ \pi^-$  pairs, but its contribution was 1) small enough (less than .5% from  $\pi^+ \pi^-$ ), 2) had a non-resonant energy dependence and so could not affect the interference curve. The number of collinear events detected in the background runs was proportional to the measurement time and independent of the beam parameters. All their features were typical of cosmic ray events. They contributed practically only to muons at a level of about 1:330 that is negligibly small.

After all cuts the ratio between  $e^+ e^-$ ,  $\mu^+ \mu^-$  and  $\pi^+ \pi^-$  became

$$31:1.9:1.$$

These events were separated into three groups in the following way. The events with both particles stopped inside the shower-range system formed the first group called a "short-range" one. Another group named "long-range" included events where both particles went through all five shower-range chambers (total range about  $180 \text{ g/cm}^2$  of Fe). All other events came into a "mixed" group. The distribution of  $e^+ e^-$ ,  $\mu^+ \mu^-$  and  $\pi^+ \pi^-$  over the three groups is presented in Table 1.

	$e^+ e^-$	$\mu^+ \mu^-$	$\pi^+ \pi^-$	$ee : (\mu\mu + \pi\pi)$	$\mu\mu : \pi\pi$
Short range	100%	.5%	83%	36:1	1:90
Mixed	.14%	12.5%	16.3%	1:9	1.5:1
Long range	$5 \cdot 10^{-5}\%$	87%	.7%	$1:10^5$	238:1

Table 1

Taking into account this distribution further selection was done in the following way. All long-range events were considered to be mesons ( $\mu + \pi$ ). The short range and (separately) mixed events were divided with the help of sandwich signals into mesons and electrons. A special parameter constructed for this purpose was a ratio of the amplitude likelihood functions for electrons and mesons. Two values of this parameter (for the two particles detected) in each event filled two-dimensional correlation matrix, enabling further separation. Short range events came only from two processes;  $e^+e^-$  and  $\pi^+\pi^-$  (see Table 1). In this case the correlation matrix method /5/, which we often used before, worked well. For mixed events the same method was slightly modified. Meson number determination in this group was considerably easier because of a small part of electrons in it (see Table 1).

After receiving the meson numbers in each of the three groups it was possible to obtain the number of muons and pions separately. For this purpose the probability (about 93%) for muon to have a full range was used which had been obtained in Monte-Carlo simulation. It was the only Monte-Carlo information necessary for the separation procedure. The pion full range probability (about 8%) was calculated from the same equations as pion and muon numbers. It was also compared with a Monte-Carlo prediction /6/. The muon probability used depends mainly on the two rather simple for Monte-Carlo processes: ionization losses and multiple scattering. Their correct simulation was additionally checked. As a result of analysis the number of electrons  $N_{ee}$ , muons  $N_{\mu\mu}$  and pions  $N_{\pi\pi}$  were obtained in each energy point of all three scanning cycles which were analyzed up to date. Total number of different type events in the present analysis ( $\sim 60\%$  of the data taken) was:

$$\begin{aligned} N_{ee} &= 205608 \\ N_{\mu\mu} &= 12708 \\ N_{\pi\pi} &= 6689 \end{aligned}$$

Besides, some noncollinear events due to the reactions  $e^+e^- \rightarrow \varphi \rightarrow K_L K_S$  and  $\rightarrow \pi^+\pi^-$

$e^+e^- \rightarrow \varphi \rightarrow \pi^+\pi^-\pi^0$  were selected and analyzed as described in /3/. Using the  $\varphi$ -meson excitation curve in these channels,  $\varphi$ -meson parameters were obtained. Then taking the  $\varphi$ -meson mass value from /3/, absolute calibration of energy scale was performed. The calibration was done for each scanning cycle separately. The parameters of interference between resonant processes

$$\begin{aligned} e^+e^- \rightarrow \varphi \rightarrow \mu^+\mu^- \\ e^+e^- \rightarrow \varphi \rightarrow \pi^+\pi^- \end{aligned}$$

and corresponding nonresonant ones were first obtained for each scanning cycle separately. They appeared to be statistically consistent and three cycles were summed up. Below throughout the paper only total statistics will be referred to. The detection cross-section of

$$e^+e^- \rightarrow M^+M^-$$

where  $M$  - stands for  $\mu$  or  $\pi$  may be written with  $\varphi$ -contribution in a form

$$\sigma_{MM}(E) = \sigma_{MM}^0(E) \cdot \left| 1 + \sqrt{\frac{\sigma_\varphi B_M}{\sigma_{MM}^0(M_\varphi/2)}} e^{i\psi} \frac{M_\varphi \Gamma_\varphi}{4E^2 - M_\varphi^2 + iM_\varphi \Gamma_\varphi} \right|^2 \quad (1)$$

Here  $E$  is the beam energy,  $M_\varphi$  and  $\Gamma_\varphi$  -  $\varphi$ -meson mass and width,  $\sigma_\varphi$  - cross-section of  $\varphi$ -meson production by  $e^+e^-$ ,  $B_M$  - branching ratio of  $\varphi \rightarrow M^+M^-$ ,  $\psi$  - phase,  $\sigma_{MM}^0(E)$  - nonresonant detection cross-section. For pions, nonresonant cross-section may contribute in a more complicated way than in (1), but it corresponds to some renormalization of  $B_M$ . Some processes like

$$e^+e^- \rightarrow \varphi \rightarrow K\bar{K} \rightarrow \rho \rightarrow \pi^+\pi^-$$

may result in a slightly different form of the cross-section but we checked this effect to be negligible at our statistics. Finally, the energy dependence of  $\Gamma_\varphi$  is ignored in (1) but its influence on the results is also very weak.

Radiative corrections lead to

$$\sigma_{MM}(E) \rightarrow \int_0^{E_{cr}} \sigma_{MM}(\sqrt{E(E-E_x)}) \cdot P(E, E_x) dE_x$$

where  $P(E, E_x)$  is the emission probability of photon with energy  $E_x$ . When  $B = \sqrt{\sigma_\phi B_M / \sigma_{MM}(M_\phi/2)} \ll 1$  the corrections connected with  $\sigma_{MM}^0(E)$  and another part of the expression (1) may be separated. That means that radiatively corrected cross-section may be written as:

$$\sigma_{MM}(E) \cdot (1 + \delta_0(E)) \cdot (1 + \delta_\phi(E))$$

Here  $\delta_0(E)$  is a nonresonant correction which may be expressed as follows:

$$\delta_0(E) = [\sigma_{MM}^0(E)]^{-1} \cdot \int_0^{E_{cr}} \sigma_{MM}^0(\sqrt{E(E-E_x)}) \cdot P(E, E_x) dE_x - 1$$

It takes into account the violation of collinearity when  $E_x > E_{cr}$  (the integration over the detection solid angle is implied) and the smooth energy dependence of  $\sigma_{MM}^0(E)$ . In the energy interval of our scanning  $\delta_0(E)$  may be supposed to be constant. On the contrary, the  $\delta_\phi(E)$  correction function is due only to the  $\phi$ -meson contribution and may be defined as:

$$\delta_\phi(E) = \left[ R(E) \cdot \int_0^{\bar{E}_{cr}} P(E, E_x) dE_x \right]^{-1} \cdot \int_0^{\bar{E}_{cr}} R(\sqrt{E(E-E_x)}) \cdot P(E, E_x) dE_x - 1$$

$$\text{where } R(E) = \left| 1 + B \cdot e^{i\psi} \frac{M_\phi \Gamma_\phi}{4E^2 - M_\phi^2 + iM_\phi \Gamma_\phi} \right|^2$$

and  $\bar{E}_{cr}$  is the mean energy  $E_{cr}$  which in our case is about 40 MeV. ( $\bar{E}_{cr} \gg \Gamma_\phi$  and its value does not influence  $\delta_\phi(E)$  notably). This correction "smooths" down the interference wave and it differs from zero in the several  $\Gamma_\phi$  vicinity of the  $\phi$ -mass. It depends on  $B$  and  $\psi$ , and provided  $B \ll 1$  it is easy to show that  $B$  dependence of  $\delta_\phi$

is almost linear

$$\delta_\phi(E, B, \psi) \approx B \cdot \delta_\phi'(E, \psi)$$

where  $\delta_\phi'$  no longer depends on  $B$ .

To fit the experimentally measured quantities  $N_{\mu\mu}/N_{ee}$  and  $N_{\pi\pi}/N_{ee}$  the same parametrization form based on aforesaid was used:

$$\frac{N_{MM}}{N_{ee}} = g_M \cdot K \cdot (F_0 + A(E - M_\phi/2)) \times \left| 1 + \sqrt{\frac{3}{4}} \frac{B_e B_M}{g_M F_0} \frac{e^{i\psi}}{\chi + i} \right|^2 \times \left( 1 + \sqrt{\frac{3}{4}} \frac{B_e B_M}{g_M F_0} \delta_\phi'(E, \psi) \right)$$

Here  $\chi = (4E^2 - M_\phi^2) / M_\phi \Gamma_\phi$ ,  $B_e$  - branching ratio of  $\phi \rightarrow e^+e^-$ ,  $g_M$  - factor which is equal to  $d^2/12$  for muons and to  $(d^2/12) \cdot (\beta_\pi^2(M_\pi/2)/4)$  for pions,  $F_0$  - absolute value of meson form-factor squared and  $A$  - its slope at the  $\phi$ -mass point, (for muons  $F_0 = 1$ ,  $A = 0$ ),  $K$  - coefficient including the detection efficiencies and "smooth" radiative corrections for mesons and electrons. The following values of  $\phi$ -parameters were used [7]:

$$\Gamma_\phi = 4.1 \text{ MeV}$$

$$B_e = 3.1 \cdot 10^{-4}$$

Radiative correction function  $\delta_\phi'(E, \psi)$  in the case of muons was calculated for  $\psi = 0$ . For pions the optimal phase  $\psi_0$  without this correction had been first obtained. Then the  $\delta_\phi'(E, \psi_0)$  was used.

Experimental results for  $N_{\mu\mu}/N_{ee}$  and  $N_{\pi\pi}/N_{ee}$  are given at fig. 2b) and 2c) with the best fit curves. As an example at fig. 2a shown is the  $\phi$ -meson excitation curve used for absolute calibration of the energy scale for one scanning cycle. We start the discussion of the results with the process



In this case we fixed  $F_0 = 1$ ,  $A = 0$ ,  $\Psi = 0$  and  $B_e$  which is known with high accuracy

$$B_e = (3.1 \pm .1) \cdot 10^{-4}$$

The parameters  $K$  and  $B_\mu$  remained free through the fit. For the first one it was obtained

$$K = (1.36 \pm .02) \cdot 10^4$$

that is consistent with the value expected from Monte-Carlo simulation

$$K_{MC} = (1.38 \pm .06) \cdot 10^4$$

The optimal value for  $B_\mu$

$$B_\mu = (4.5 \pm 1.0) \cdot 10^{-4}$$

does not contradict to the expected equality  $B_\mu = B_e$ . The value of  $P(\chi^2)$  for the curve at fig. 2b) is 7.9%.

In the fit for  $N_{\pi\pi}/N_{ee}$  we fixed

$$B_e = 3.1 \cdot 10^{-4} \quad \text{and}$$

$$F_0 = 2.6 \quad \text{from our previous}$$

work /2/. The parameters  $B_\pi$ ,  $\Psi$ ,  $A$  and  $K$  remained free. The additional restriction was imposed on  $A$  from our previous work /8/ where  $|F_\pi|^2$  had been measured in a wide energy region. Using  $|F_\pi|^2$  values for the  $2E = 980 - 1050$  MeV interval from /8/ we obtained for  $A$

$$A = (-2.3 \pm 1.8) \cdot 10^{-2} \text{ MeV}^{-1}$$

This restriction was included in the likelihood function for  $N_{\pi\pi}/N_{ee}$ .

Optimal  $K$  value

$$K = (1.29 \pm .03) \cdot 10^4$$

is consistent with that obtained in Monte-Carlo simulation

$$K_{MC} = (1.31 \pm .08) \cdot 10^4$$

At fig. 3  $\chi^2$  versus  $B_\pi$  with  $\Psi$ ,  $A$  and  $K$  remained free is plotted. The straight line shows a 68% confidence interval. The optimal value for  $B_\pi$  is

$$B_\pi = 1.0^{+.8}_{-.5} \cdot 10^{-4}$$

The minimum  $\chi^2$  is 20.5 for 15 degrees of freedom, that gives  $P(\chi^2) = 15\%$ . Nonresonant  $|F_\pi|^2$  is shown at fig. 2c) as a solid straight line. If  $B_\pi$  is put to be zero, the  $\chi^2$  value becomes by 9 units larger than for optimal  $B_\pi$ . This shows that optimal  $B_\pi$  is at the distance of three standard deviations from zero. In the other words the probability of such a fluctuation for  $B_\pi = 0$  is of order  $10^{-3}$ . The latter statement was checked by special Monte-Carlo simulation. The optimal form-factor for  $B_\pi = 0$  is shown at fig. 2c) by a dashed line.

Optimal value for phase  $\Psi$  is equal

$$\Psi = -13^\circ \pm 20^\circ$$

The best upper limits on  $B_\pi$  existing before this experiment are:

$$B_\pi < 2.7 \cdot 10^{-4} \quad (95\% \text{ c.l.}) \quad /9/$$

$$B_\pi < 4.0 \cdot 10^{-4} \quad (95\% \text{ c.l.}) \quad /10/$$

In conclusion the authors express their sincere gratitude to A.I.Vainshtein and V.M.Budnev for the fruitful discussions and useful remarks.

## References

1. G.M.Tumaikin. Proceed. of the X International Conference on High Energy Accelerators, Serpukhov, 1977, vol. 1, p. 443.
2. A.D.Bukin et al., Yadernaya Fizika, 27 (1978) 985.
3. A.D.Bukin et al., Yadernaya Fizika, 27 (1978) 976.
4. V.M.Aulchenko et al., Preprint INP 79-65, Novosibirsk, 1979.
5. A.D.Bukin et al., Preprint INP 77-92, Novosibirsk, 1977.
6. A.D.Bukin, S.I.Eidelman, Preprint INP 77-101, Novosibirsk, 1977.
7. Particle Data Group, Phys. Lett., 75B (1978).
8. A.D.Bukin et al., Phys. Lett., 73B (1978) 226.
9. H.Alvensleben et al., Phys. Rev. Lett., 28 (1972) 66.
10. S.Jullion, Proceedings of the XVIII International Conference On High Energy Physics, vol. 2, p. B 19.

In this paper we present the preliminary results on the search of  $\Phi(1020) \rightarrow \pi^+\pi^-$  decay. Experimentally this decay had not yet been observed. The measurements were performed at the end of 1977 - beginning 1978 with the "OLYA" detector at the electron-positron storage ring VEPP-2M /1/. After our previous experiment /2/ on the search of this decay in 1975 the second stage of the detector "OLYA" was completed. It includes a set of shower-range spark chambers allowing in particular muon-pion separation. On the other hand, the storage ring luminosity increased considerably enabling us to collect  $\sim 20$  times larger statistics. Up to the moment about 60% of data have been analyzed.

The "OLYA" detector described elsewhere /3/ consists of four identical quadrants surrounding the interaction region. The useful solid angle of the detector is  $.65 \cdot 4\pi$  steradian. Each quadrant contains:

- a set of scintillation counters for triggering and timing,
- four two-dimensional wire spark chambers for measurement of coordinates of charged particles tracks,
- sandwich of four scintillation counters as a shower detector,
- five two-gap shower-range spark chambers for measurement of charged particle ranges and  $\gamma$  - quanta coordinates.

The readout is completely digitized with the "M-6000" mini-computer on-line. The detailed description of the detector may be found in /4/.

The experiment was carried out as four completely independent scannings of the  $\Phi$  -meson region with a total energy step  $\Delta(2E) = .5$  MeV, approximately equal to the c.m.s. energy spread. The integrated luminosity was  $\approx 900 \text{ nb}^{-1}$ , total measurement period - about a month and a half, pure measurement time -  $1.26 \cdot 10^6$  sec. The luminosity was determined by Bhabha scattering at large angles. Runs with beams colliding in another interaction region were made to study single beam background. Cosmic ray background was measured in the



special runs without any beams in the ring.

Data analysis included the selection of two-track events with particles being collinear

$$|\Delta\varphi| < 2^\circ \quad \sigma_{\Delta\varphi} \approx .8^\circ$$

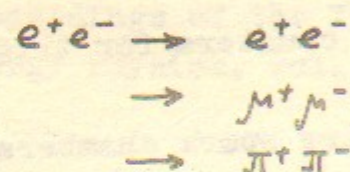
$$|\Delta\theta| < 3^\circ \quad \sigma_{\Delta\theta} \approx 1.2^\circ$$

and coming out of the beam region

$$|DY| < 4\text{mm} \quad \sigma_{DY} \approx 1\text{mm}$$

$$|DZ| < 4\text{mm} \quad \sigma_{DZ} \approx 1\text{mm}$$

Additional selection was done by the time-of-flight and the standard beam bunch timing. Events thus selected came mainly from the processes:



Charged kaons from



had in the  $\Phi$  - region too small kinetic energy to trigger the system.

The rough preliminary analysis showed the ratio of  $e^+e^-$ ,  $\mu^+\mu^-$  and  $\pi^+\pi^-$  pairs to be about

$$25 : 1.5 : 1.$$

It also revealed the characteristic signals from these three processes in the detector allowing their final separation.

The main background to  $e^+e^- \rightarrow \pi^+\pi^-$  in our case came from  $e^+e^- \rightarrow \Phi \rightarrow K_L K_S \rightarrow \pi^+\pi^-$ . The pions from  $K_S$  decays gave at the  $\Phi$  - maximum about 2.5% of the selected  $\pi^+\pi^-$  events. The characteristic feature of this back-

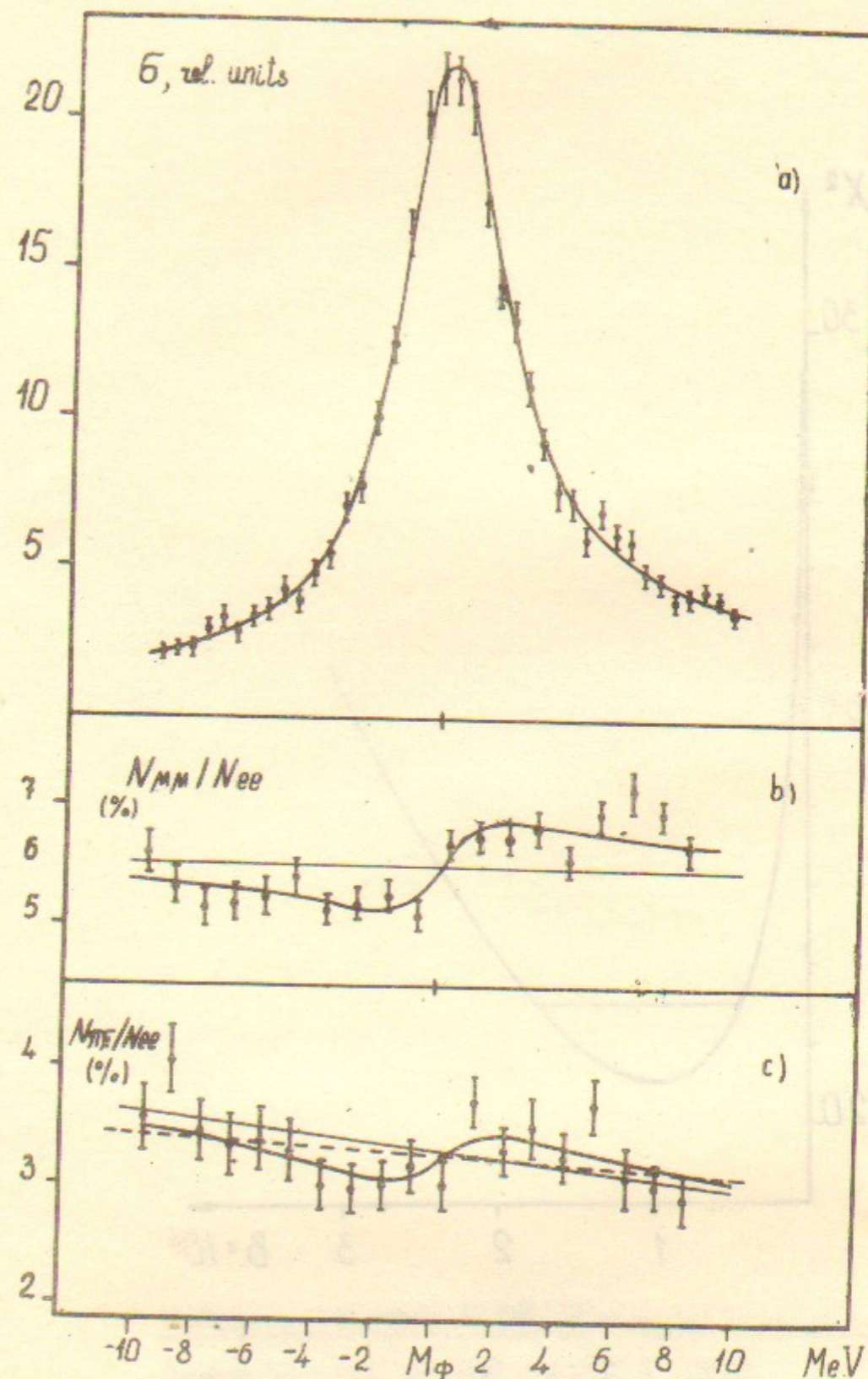


Fig 2.

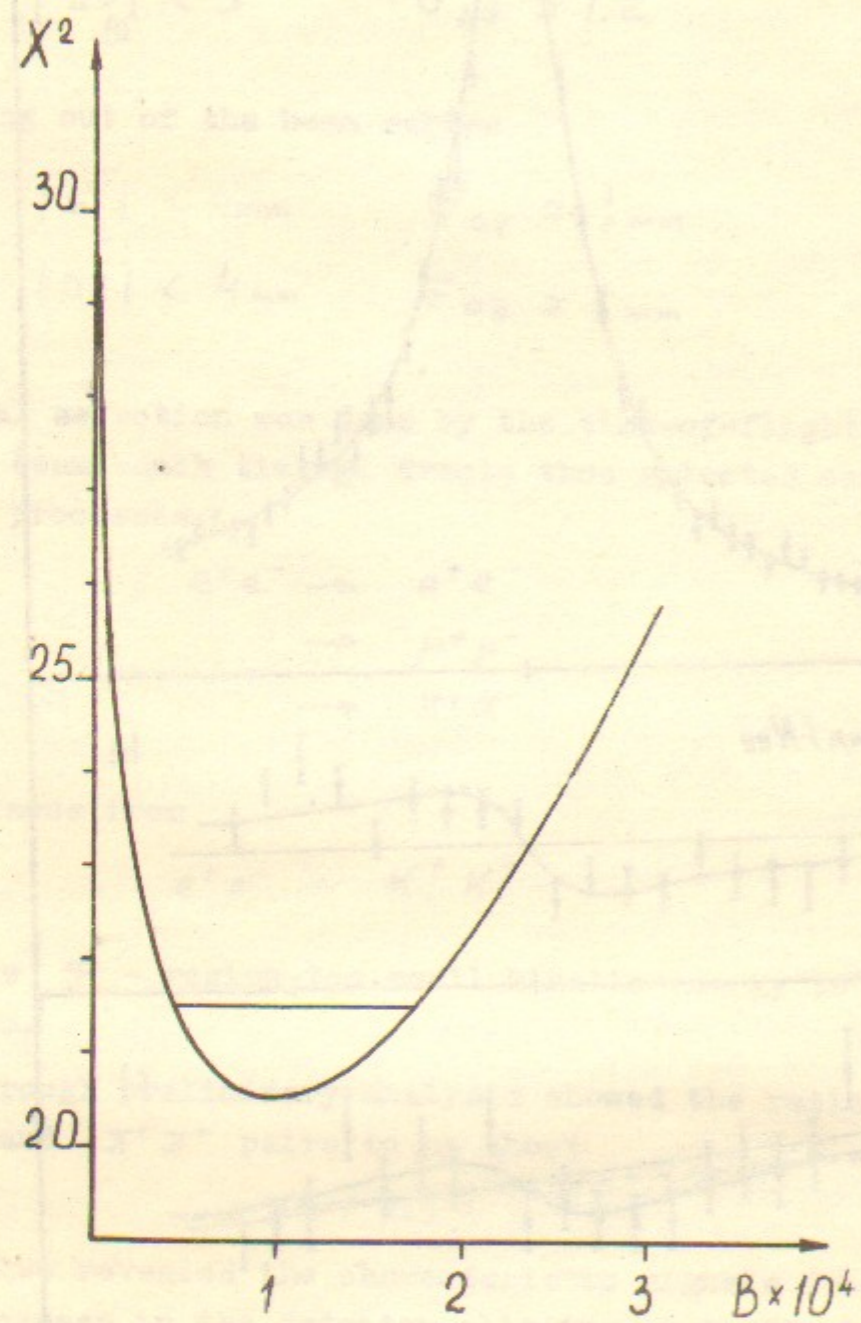


Fig 3.

Работа поступила 8.08.79 г.

Ответственный за выпуск - С.Г.ПОПОВ  
 Подписано к печати 15.08.79г. МН 02976  
 Усл. I, I печ.л., 0,9учетно-издл.  
 Тираж 200 экз. Бесплатно.  
 Заказ № 66

Отпечатано на ротапринте ИЯФ СО АН СССР